Regulation of kappa opioid receptor inactivation depends on sex and cellular site of antagonist action

Kathryn L. Reichard[1,2,3], Keionna A. Newton[1,2], Zeena M.G. Rivera[1,2], Paulo M. Sotero de Menezes[1,2], Selena S. Schattauer[1,2], Benjamin B. Land[1,2], Charles Chavkin[1,2,3].

[1]Neurobiology of Addiction, Pain, & Emotion, [2]University of Washington Department of Pharmacology, [3]University of Washington Graduate Program in Neuroscience, Seattle, WA 98195

Running Title: JNK dependent inactivation of KOR

Address correspondence to:
  Dr. Charles Chavkin
  Department of Pharmacology, Box 357750
  University of Washington School of Medicine
  Seattle, WA 98195-7750

  206 543 4266 (v)
  cchavkin@uw.edu

Text Pages: 10 single-spaced, Times New Roman
Abstract: 239 words
Introduction: 610 (650 with citations)
Discussion: 1017 words

Abbreviations: KOR (Kappa Opioid Receptor), norbinaltorphimine (norBNI), G-protein receptor kinase (GRK), cJun Kinase (JNK), p38 mitogen-activated protein kinase (p38 MAPK), reactive oxygen species (ROS), Compound 101 (CMPD101), artificial cerebrospinal fluid (aCSF), maximum possible effect (MPE), ventral tegmental area (VTA), nucleus accumbens (NAc), Dopamine Transporter (DAT), G Protein-coupled inwardly rectifying potassium (GIRK) channel, β-chlornaltrexamine (β-CNA), nlx (naloxone)

Keywords: antidepressant drug development, GPCR regulation, sex-differences in drug response

ABSTRACT

The prototypical member of the receptor-inactivating kappa opioid receptor (KOR) antagonists norbinaltorphimine (norBNI) produces prolonged receptor inactivation by a cJun kinase mechanism. These antagonists have potential therapeutic utility in the treatment of stress-disorders, however additional preclinical characterization is necessary to understand important aspects of their action. In this study, we report that norBNI does not work as effectively in female mice as in males because of estrogen regulation of G-protein receptor kinase (GRK); pretreatment of ovary-intact female mice with the selective GRK2/3 inhibitor, CMPD101, made females equally sensitive to norBNI as males. Prior observations suggested that *in vivo* treatment with norBNI does not produce long-lasting inhibition of KOR regulation of dopamine release in the nucleus accumbens. We assessed the persistence of norBNI receptor inactivation in subcellular compartments. Fast-scan cyclic voltammetry recordings confirmed that presynaptic inhibition of dopamine release by the KOR agonist U69,593 was not blocked by *in vivo* pretreatment with norBNI under conditions that prevented KOR mediated aversion and analgesia. We employed a novel *in vivo* proxy sensor of KOR activation, AAV-DIO-HyPerRed and demonstrated that KOR activation stimulates JNK-dependent ROS production in somatic regions of VTA dopamine neurons, but did not activate ROS production in dopamine terminals. The compartment selective action helps explain how dopamine somatic, but not terminally expressed KORs are inactivated by norBNI. These results further elucidate molecular signaling mechanisms mediating receptor-inactivating KOR antagonist action and advance medication development for this novel class of stress-resilience medications.

SIGNIFICANCE STATEMENT

Kappa opioid receptor (KOR) antagonists are being developed as novel pro-resilience

therapeutics for the treatment of mood and substance use disorders. This study showed that the

long-acting KOR antagonists are affected by both the sex of the animal and the subcellular

compartment in which the receptor is expressed.

INTRODUCTION

Prolonged or severe behavioral stress exposure increases risk of mood and substance use disorders (Kessler et al., 1997; Gold et al., 2002; Gold, 1998; Koob et al., 2008). The release of endogenous opioid dynorphin peptides throughout the brain contributes to these adverse behavioral effects (Ehrich et al., 2015; Abraham et al., 2018a). For this reason, researchers have explored using kappa opioid antagonists as antidepressants and anti-addiction therapeutics in both pre-clinical research and human clinical trials (Buda et al., 2015; Carrol & Carlezon, 2013; Lowe et al., 2014; Chavkin et al., 2019). Three different forms of KOR antagonists have been identified: nonselective (e.g. buprenorphine and naltrexone) (Leander, 1988), selective long-acting receptor inactivating compounds (e.g. norBNI and JDtic) (Bruchas et al., 2007; Melief et al., 2011), and selective competitive antagonists (e.g. LY2456302 and BTRX-140) (Rorick-Kehn et al., 2014; Guerrero et al., 2019). There are theoretical advantages and disadvantages to each antagonist type, and it has yet to be determined which avenue is best to pursue for clinical development. The advantages of receptor-inactivating compounds include the ability to produce a stable effect with less concerns about patient compliance, however, several observations about their mechanism must be resolved before moving forward with the development of this class of medications.

A recent study showed that there is a sex difference in JNK activation by norBNI in C57BL6-J mice (Laman-Maharg et al., 2018). This work also demonstrated that in female C57BL6-J mice, pretreatment with norBNI does not reduce immobility in the forced swim test, in contrast to its effects in males. In addition to published concerns about effectiveness in female mice, we also noted that norBNI was not persistently antagonizing KOR inhibition of dopamine release when

5

used in *in vitro* voltammetry assays of dopamine release (unpublished observations). In order to understand and resolve these issues, we measured sex differences in response to norBNI and clarified the mechanisms responsible for its long-lasting effects on KOR function (Abraham et al., 2018b; Becker et al., 2019).

The prototypical receptor-inactivating KOR antagonist norBNI has a long duration of action *in vivo* with effects lasting 14-21 days, but the drug does not persistently or covalently bind to the receptor (Smith et al., 1990; Horan et al., 1992; Butelman et al., 1993). Instead, norBNI has been demonstrated to disrupt KOR-signaling by selectively activating a c-Jun Kinase (JNK) signaling cascade which activates the phospholipase PRDX6 and subsequently stimulates the generation of reactive oxygen species (ROS) through an NADPH-oxidase mechanism (Bruchas et al., 2007; Schattauer et al., 2017a; Fisher, 2011). Local ROS production oxidizes the $G\alpha_i$ subunit at a critical cysteine palmitoylation site, disrupts G protein-receptor interaction, and thus prevents agonist-dependent guanine nucleotide exchange (Schattauer 2017a). This KOR-inactivating process can be blocked by inhibitors of JNK or the PLA2 activity of PRDX6 and can be detected with ROS sensors, including the genetically encoded indicator HyPerRed fluorescent protein indicator which sensitively reports production of hydrogen peroxide (Schattauer et al., 2017a; Schattauer 2019). ROS-dependent inactivation of KOR can be produced by administering a single high dose of norBNI, or by administering repeated low doses of norBNI (Chavkin et al., 2019). This action is due to collateral agonist activity, an effect wherein a compound acts as an antagonist by selectively activating a subcomponent of receptor signaling, in turn inactivating subsequent signaling at that receptor (Kenakin, 2005; Bruchas et al., 2007). NorBNI's collateral agonist activity led us to hypothesize that the long-lasting effect is likely sensitive to sex

hormone regulation, and may be subject to signaling differences between different cell-types and subcellular compartments.

In this study, we explored the constraints of norBNI's antagonist activity and assessed the persistence and subcellular localization of JNK-ROS mediated receptor inactivation. We confirmed that norBNI is not a consistently effective long-acting antagonist in female mice, nor does it consistently increase phospho-JNK in female mice. We found that its phosphorylation of JNK and long-acting antagonist activity can be restored with the GRK2/3 inhibitor Compound101 (CMPD101), and that repeated, low-doses of norBNI produced long-lasting antagonist effects in female mice. We also demonstrated that norBNI was not an effective long-acting antagonist at VTA dopamine terminals, but did block KOR-activation in VTA cell bodies. KOR activated potassium (GIRK) currents in VTA dopamine neurons were inhibited one-week post norBNI-injection. Consistent with prior mechanistic studies of receptor inactivation, we found KOR activation of ROS was evident in VTA dopamine cell bodies but not in the axons and terminals of dopamine neurons. These findings indicate that the pharmacological actions of norBNI depend on sex and cellular site of action.

METHODS

Animals

Drug- and procedure-naïve C57BL/6-J mice (adult, male 20–30 g, female 17-25g; bred for multiple generations after sourcing from Jackson Labs) were group housed on a 12 h light/dark cycle with food and water ad libitum. Animal procedures were approved by the Animal Care and Use Committee of the University of Washington and conform to the

guidelines on the care and use of animals promulgated by the National Institutes of Health.

Mice expressing Cre-recombinase under the control of the endogenous dopamine transporter

locus (*Slc6a3*[IRES-Cre] or DAT-IRES-Cre) were used for viral injections (Zhuang et al., 2005).

Drugs

U69,593 ((+)-(5α,7α,8β)-N-Methyl-N-[7-(1-pyrrolidinyl)-1-oxaspiro[4.5]dec-8-yl]-

benzeneacetamide) (NIDA Drug Supply) was dissolved in solvent (DMSO) to 1 mM stocks and

stored at -20˚C for up to one month. β-chlornaltrexamine dihydrochloride (β-CNA) (Sigma-

Aldrich) was dissolved 1 µg/µl in saline and stored at -20˚C for up to one month. U50,488 (2-

(3,4-dichlorophenyl)-*N*-methyl-*N*-[(1*R*,2*R*)-2-pyrrolidin-1-ylcyclohexyl]acetamide, NIDA Drug

Supply) was dissolved in 1 mg/mL saline prior to IP injection to 10 mg/kg for tail flick.

Norbinaltorphimine (norBNI, NIDA Drug Supply) was dissolved 1 mg/mL in saline prior to IP

injection unless stated otherwise. CMPD101 (3-[[[4-Methyl-5-(4-pyridinyl)-4*H*-1,2,4-triazol-3-

yl]methyl]amino]-*N*-[[2-(trifluoromethyl)phenyl]methyl]benzamide; Tocris) was dissolved at 1.5

mg/mL in 10% ethanol/10% cremophor/80% saline prior to IP injections. CMPD101 and norBNI

were delivered in IP injections of 10 ml/1 kg of body weight to doses of 15 mg/kg and 10 mg/kg,

respectively. Nalfurafine hydrochloride ((2*E*)-*N*-[(5α,6β)-17-(cyclopropylmethyl)-3,14-

dihydroxy-4,5-epoxymorphinan-6-yl]-3-(3-furyl)-*N* methylacrylamide) (NIDA Drug Supply)

was dissolved in sterile water at 100 µM and stored at -20˚C.

Behavioral Assays

Female mice were tested for latency (in seconds) to withdraw tail (flick) from 52.5°C water to

assess anti-nociceptive effects of KOR activation (Bruchas et al., 2007). Mice were tested for

basal latency to flick and treated with CMPD101 (15 mg/kg, i.p.), then tested 30 min later and

treated with U50,488 (10 mg/kg, i.p.) and retested for latency to flick 30 min later. For repeated

low-dose norBNI pre-treatment, female mice received one injection of norBNI (1 mg/kg, i.p.) or

an equivalent volume of saline daily for seven days prior to the tail withdrawal assay. For

CMPD101 and norBNI pre-treatment, female mice received CMPD101 (15 mg/kg, i.p.) and

thirty minutes later, received norBNI (10 mg/kg, i.p.) or an equivalent volume of vehicle or

saline, respectively, seven days prior to the tail withdrawal assay.

Stereotaxic Surgery (ICV) Mice were anesthetized with isoflurane and mounted on a model

1900 stereotaxic alignment system (David Kopf Instruments). β-CNA was loaded into a

Hamilton Syringe and delivered at a rate of 200 nl/min into the lateral ventricles (Coordinates:

A/P +0.3, M/L +0.8, D/V -3.0 *or* A/P -0.5, M/L +1.0, D/V -2.5) (Paxinos & Franklin, 2008;

Devos & Miller, 2013). Two coordinates were used to avoid excess bleeding because of

divergent location of skull sutures. An adenovirus associated double floxed inverted (AAV-DIO)

virus was generated containing the genetically encoded ROS sensor HyPerRed (Schattauer et al.,

2019; Ermakova et al., 2014). AAV-DIO HyPerRed virus was injected into the VTA of DAT-

IRES-Cre heterozygous mouse (Coordinates: A/P -3.3, M/L +/- 0.5, D/V -4.4) so that the

HyPerRed sensor would be expressed exclusively in dopamine neurons expressing Cre

recombinase.

Fast-Scan Cyclic Voltammetry

Mice were decapitated and the head placed in pre-oxygenated, cold modified artificial

cerebrospinal fluid (aCSF) (248 mM sucrose was substituted for NaCl). The brain was removed,

and 250 μm coronal slices containing nucleus accumbens were prepared (Leica, model VT-1000X). Nucleus accumbens slices were transferred to standard oxygenated aCSF (124 mM NaCl, 2.5 mM KCl, 1.25 mM 12 NaH$_2$PO$_4$, 1.25 mM MgSO$_4$, 2 mM CaCl$_2$, 10 mM dextrose, 25 mM NaHCO$_3$) and incubated for 1 hr at 37° C, then held at room temperature before recordings. Slices were placed in a recording chamber, and perfused with oxygenated aCSF at 31-33°C throughout recording. Carbon-fiber working electrodes were fabricated as described (Clark et al., 2010; Lemos et al., 2012), hand-cut to 150-200 μm past the capillary tip. A single electric pulse (120-200 μA, 2 ms per phase) was applied to a parallel bipolar stimulating electrode to evoke dopamine release, and the potential at the working electrode was held at -0.4V versus Ag/AgCl, ramped to +1.3V and back to -0.4V at a rate of 10 Hz. Baseline dopamine release was measured every 2 min for 20 min prior to measuring release in response to 100 nM U69,593. Waveform generation, data acquisition and analysis were carried out using two PCI multifunction data acquisition cards and software written in LabVIEW v7.1 (National Instruments, Austin, TX) as described (Clark et al., 2010; Lemos et al., 2012). Responses in the last 8 min (4 recordings) were averaged to calculate the U69,593 response.

Electrophysiology Horizontal VTA slices were prepared using the N-Methyl D-Gluconate (NMDG) GaCSF and HEPES solutions previously described (Ting et al., 2014). To record VTA G protein gated inwardly rectifying potassium channel (Kir3, GIRK) currents, the resistance of the electrodes was 3–7 MΩ when filled with an internal solution of (mM) K-gluconate 130, NaCl 5, Na phosphocreatine 10, MgCl$_2$ 1, EGTA 0.02, HEPES 10, MgATP 2, Na$_2$GTP 0.5, 0.1% Biocytin, pH 7.3. Whole cell voltage clamp recordings were performed on neurons in the VTA expressing tdTomato reporter expressed only in DAT-expressing neurons. The cell was voltage

clamped at −60 mV using an Axopatch 200B amplifier (Molecular Devices, Foster City, CA).

Signals were digitized by a Digidata 1440 A/D converter (Molecular Devices) and stored using

pClamp 10.2 software (Molecular Devices). To record GIRK currents, once a cell was stably

patched and basal physiology assessed, the slice was bathed in high potassium (5.5 mM

K^+) ACSF to enhance the currents in the cells at hyperpolarized potentials. As expected, when

the slice was incubated in high [K^+], the holding current increased and inward rectification was

more apparent. The membrane potentials of VTA neurons were subjected to a voltage ramp

protocol in which they were brought from −120 mV to −50 mV over 10 sec. After three stable

ramp measurements (the average of three sweeps) were obtained, U69,593 (1 μM) was bath

applied and the slice was allowed to equilibrate for 3 min. Subsequently, a ramp measurement

was taken after 12 min of U69,593 application and the three sweeps were averaged. Following

U69,593 application and stable current responses, $BaCl_2$ (100 μM) was added to distinguish Ba^{2+}-

sensitive GIRK currents.

Conductance was calculated as the slope of the I-V curve in response to a voltage ramp from

-120 mV to -50 mV. Maximal inward current was calculated as the average current in response

to a -115 mV applied voltage.

HyPerRed Imaging and Analysis VTA slices were prepared as described above for the slice

recordings. Modified aCSF solution included 800 μM thiourea and 400 μM sodium ascorbate

(Rice, 1999) to reduce cellular stress and keep basal ROS levels low. Agonist-induced ROS

HyPerRed fluorescence was recorded on an upright fluorescent microscope (Olympus BX51WI),

with the fluorophore excited by CoolLED pE300 through the 20x objective at 555 nm and

collected using an Hammamatsu ORCA-Flash4.0 V2 camera and HC Image Live software.

Images were collected every 2 min with an exposure time of 100 ms to 500 ms and LED

intensity of 50%. For nalfurafine experiments, 35 images were taken over 70 minutes. aCSF was

washed on for 15 min, aCSF containing nalfurafine (100 nM) was washed on for 45 minutes, 200

μM H_2O_2 was added for the final 10 min (images 31-35). For naloxone-nalfurafine experiments,

40 images were taken over 80 min to establish a secondary baseline of aCSF plus naloxone (1

μM), prior to wash-on of aCSF with both naloxone *and* nalfurafine. $\Delta F/F$ was calculated as the

current fluorescence minus the average fluorescence of the four images prior to nalfurafine

("baseline fluorescence"), divided by the baseline fluorescence. Inclusion criteria required that

cells significantly increase $\Delta F/F$ at the end of experiment in response to H_2O_2 (100 μM)

application. Due to mild bleaching over the course of the experiment, a "Baseline2" was

calculated as the average of the 2 images prior to H_2O_2 wash on. Any image that did not show a

fluorescence increase of at least 5% in response to H_2O_2 was excluded from this study, as in

these cases we could not confirm functional protein expression or tissue viability.

Striatal Dissections for Phospho-JNK Western Blot Mice were decapitated at the specified

times following drug administration. Ventral striata were dissected and homogenized with a

Dounce homogenizer on ice in MAPK lysis buffer composed of 50 mM Tris-HCl, 300

mM NaCl, 1 mM EDTA, 1 mM Na3VO4, 1 mM NaF, 10% glycerol, 1% triton-X100, protease

inhibitor cocktail (Sigma-Aldrich), and phosphatase inhibitor cocktail (Millipore). Samples were

centrifuged 25 min at $30,000 \times g$ at 4°C. Protein concentrations in supernatant were determined

by bicinchoninic colorimetric assay (Thermo Fisher Scientific), mixed with 4× LDS buffer (10%

lithium dodecyl sulfate, 25% glycerol, pH 8.4; Thermo Fisher Scientific) supplemented with 8%

β-mercaptoethanol and stored at −20°C until analysis by western blot.

Western Blot for Phospho-JNK Samples were loaded with 20 µg of protein onto 10% Bis-Tris precast gels (Thermo Fisher Scientific) and run at 100 V for 2 h. Blots were transferred to nitrocellulose (Thermo Fisher Scientific) for 1.5 h at 30 V. The nitrocellulose was blocked with 5% BSA-TBST 1 h at room temperature and stained overnight at 4°C with rabbit anti-phospho-JNK antibody (Cell Signaling Technology, catalog number 9251, lot 27) 1:1000 and mouse anti-actin antibody (Abcam AB8226, lot GR111289-6) 1:5000 in 5% BSA-TBST. Blots were incubated in IRDye secondary antibody (LI-COR Biosciences, catalog number 926-68070, lot C50721-05 and catalog number 926-32211, lot C506602-05; 1:15,000) in 1:1 Odyssey buffer (LI-COR Biosciences) and 5% milk-TBST for 1 h at room temperature and then scanned on the Odyssey IR Imaging System (LI-COR Biosciences). Band intensity with background subtraction was measured using Odyssey software (Image Studio Lite 5.2, LI-COR Biosciences). Phosphoprotein band intensity was normalized to or actin band intensity. Data were normalized to percentage of control vehicle treated and plotted using GraphPad Prism 8.2 (GraphPad Software, Inc.). Statistical significance ($p < 0.05$) was determined by analysis of variance (ANOVA) followed by Šidák post hoc test.

Experimental Design and Statistical Analysis

All of the studies described in this report were designed to test specific *a priori* hypotheses. Behavioral and imaging data were collected and analyzed with the investigator blind to treatment. Animal numbers were as follows: tail flick, male n = 7 per group; CMPD101-norBNI n = 4-5 female mice per group; repeated n = 7 female mice per group; norBNI voltammetry n = 5-6 animals per group; β-CNA voltammetry n = 4-6 animals per group; electrophysiology n = 7-

8 animals, 7-10 cells per group; HyPerRed (4 animals per group). Sample sizes were estimated

with power analysis prior to assays, and adapted when effect size was an order of magnitude

outside of our estimations. This occurred for the HyPerRed experiment, as it was a novel

technique in which we expected lower signal to noise, however we saw a substantial signal over

baseline and ten-fold higher ΔF/F values than we predicted from pilot studies in cell culture. Due

to sex-dependent effects in norBNI action (described in Figure 1), experimental animals were all

male in Figures 2-4. Data were analyzed with Prism 7 software (GraphPad). Group differences

were determined using t tests, ANOVA, or repeated-measures ANOVA as described in the

Results. Post hoc comparisons were analyzed with Tukey's or Sidak's test. For all statistical tests,

α was set to 0.05.

RESULTS

Duration of antinociceptive action of norBNI in the tail-withdrawal assay. Male mice treated

with 10 mg/kg U50,488 show a significant increase in latency to withdraw their tails from

52.5˚C water, which was normalized to 100% of maximum possible effect (MPE). As previously

reported, a single (10 mg/kg, i.p.) injection of norBNI seven days prior to analgesic testing

blocked U50,488-mediated increase in tail flick latency in male mice (Figure 1A) (Unpaired two-

tailed t-test: $t_{2.916,18}$ p=0.0092). In contrast to male mice, U50,488 alone did not significantly

increase tail-flick latency in female mice (Figure 1B). As previously reported, the estrous state-

dependent insensitivity to U50,488 effect is caused by estradiol-stimulated GRK2/3 signaling

(Abraham et al., 2018b). Pretreatment with the GRK2/3 inhibitor CMPD101 restored sensitivity

to U50,488 in female mice (Figure 1B). We predicted that, like with neutral KOR agonist,

norBNI would not be long-acting in female mice due to its action as a biased KOR agonist

stimulating the phosphorylation of JNK. Although CMPD101 given just prior to U50,488

restores the effectiveness of the agonist, norBNI administered one week prior to CMPD101-

U50,488 treatment did not block KOR-mediated analgesia in female mice, indicating that there is

also a sex difference in norBNI sensitivity (Figure 1C). To test if estradiol-GRK2/3 signaling

was also responsible for this sex difference, we administered CMPD101 prior to norBNI

antagonist pretreatment seven days before the tail flick assay. The analgesic effects of U50,488

were blocked in mice treated with CMPD101 and norBNI, but not in those female mice treated

with norBNI alone (Figure 1C). Neither CMPD101 alone nor norBNI alone blocked CMPD101-

U50488 analgesia evident in female mice (One-Way ANOVA F = 5.316, p=0.0242; Tukey's

post-hoc CMPD101-vehicle vs. CMPD101-norBNI p=0.0215). These data suggest that, as we

predicted, the estrogen-GRK2 mechanism responsible for sex differences in KOR agonist action

previously identified (Abraham et al., 2018b) also contributes to the sex differences in norBNI

duration of action. Thus, estradiol-stimulated GRK2 sequestration of Gβγ likely disrupts norBNI

activation of JNK, thereby disrupting receptor inactivation of KOR by norBNI stimulated JNK

production of ROS (Abraham et al., 2018b, Schattauer et al., 2017a).

Repeated low-doses of norBNI produce a long-lasting antagonist effect in female mice. The

utility of a long-acting KOR antagonist in women that requires concomitant GRK2/3 inhibition

is not practical from a compliance perspective. An alternative dosing strategy might circumvent

that constraint. We hypothesized that if female mice were treated repeatedly with a low-dose of

norBNI, the cumulative effect of dosing over multiple days of their estrous cycle including

during low-estradiol phases, might produce a long-acting block of U50,488 mediated tail flick.

15

This potentially safer low-dosing strategy was previously demonstrated to be effective in males (Chavkin et al., 2019).

Female mice were injected with norBNI (1 mg/kg) or saline once per day for seven days. We subjected these mice to CMPD101-U50,488 tail flick 48 hours after the end of the week-long pretreatment. U50,488-induced analgesia was blocked by repeated norBNI, but not affected by repeated saline pretreatment (Figure 1D). There was no significant interaction, but there was a trend toward an interaction and a significant effect of pretreatment and time (Unpaired two-tailed t-test: $t_{2.607,11}$ p=0.0204).

Increase in phospho-JNK detected in female mice pretreated with CMPD101 prior to norBNI, but not in female mice treated with norBNI in the absence of CMPD101. Prior studies have demonstrated that, in male mice, norBNI stimulates pJNK in the striatum, and that this pJNK is necessary for the long-lasting effects of norBNI (Bruchas 2007). We predicted that GRK2/3 inhibition by CMPD101 would be required to replicate this norBNI-mediated pJNK in female mice, similarly to the CMPD101 pretreatment required to see the long-lasting block of tailflick described above. To test if the sex difference we see in norBNI action is due to estradiol-dependent shifts in Gβɣ sequestration, we measured the phospho-JNK immunoreactivity with Western blot in striatal protein samples taken from mice given norBNI or saline with either a vehicle or CMPD101 pretreatment (Figure 1B,C). Mice were given vehicle (80% saline, 10% cremophor, 10% ethanol) thirty minutes prior to norBNI (10 mg/kg IP in saline) or saline. After an hour, we dissected their striata, isolated protein, and measured phospho-JNK using Western blot. The norBNI alone did not cause a consistent increase over vehicle in our preliminary data (Figure 1B,C). However, pretreatment with CMPD101 (15 mg/kg in 80% saline, 10%

cremophor, 10% ethanol), prior to norBNI led to a significant increase over the CMPD101/saline

controls (Figure 1B,C) (Two-Way ANOVA: Interaction $F_{(1,28)} = 5.236$, $p = 0.0299$;

Pretreatment $F_{(1,28)} = 5.361$, $p = 0.0281$; Sidak post-hoc: saline condition $p = 0.997$, CMPD101

pretreatment $p = 0.0087$).

Collectively, these data demonstrate that norBNI acts effectively as an antagonist against KOR-

mediated analgesia in both male and female mice. However, in female mice, because high

estradiol can make norBNI less effective, KOR inactivation is only evident either after

pretreatment with CMPD101 or in mice repeatedly treated with low doses of norBNI. In

conjunction with recently published data (Chavkin et al., 2019), these results indicate that

repeated, low-dose norBNI treatment may be effective in both male and females. Due to this sex

difference, the rest of the reported results assessing the constraints of norBNI's effectiveness in

neuronal compartments, were completed in male mice.

NorBNI antagonism of KOR inhibition does not persist in dopamine terminals. KOR

expression has been shown to be required on VTA dopamine neurons for conditioned place

aversion to U50,488 (Ehrich et al., 2015). However, while studying the underlying mechanisms

involved, we consistently found that *in vivo* pretreatment with norBNI did not have long-lasting

effects on KOR regulated dopamine release as measured using slice *ex vivo* voltammetry. The

discrepancy between norBNI's long-lasting effects on KOR-dependent aversion and its lack of

long-lasting effect in vitro is surprising because the dominant theory rationalizes the KOR

aversion as a consequence of presynaptic inhibition of dopamine release (Chefer et al., 2013).

Traditional kappa opioid receptor agonists are known to generate a robust inhibition of dopamine terminals in the nucleus accumbens (Di Chiaro & Imperato, 1988*)*. To systematically establish whether presynaptic inhibition can be blocked by norBNI, C57BL/6-J mice were injected with 10 mg/kg norBNI or an equivalent volume of saline one week, 24 hours, or 1 hour prior to brain dissection and tissue sectioning (Figure 2A-D). We predicted that if norBNI was a long-lasting antagonist, inhibition of U50,488 effects on dopamine release would be evident 1 hr after in vivo administration and persist for 1 week. In contrast, we found that NorBNI acted as an effective antagonist in animals sectioned 1 hour post IP injection of norBNI, but neither 24 hour nor one-week pretreatment with norBNI was effective at blocking the U50,488 effects on evoked dopamine release (One-way ANOVA F = 8.17, p = 0.0012, Tukey's post-hoc Saline vs 1-hour p = 0.0031, Saline vs. 24 hr p = 0.8396, Saline vs. 1 week p = 0.9381). These results confirm that norBNI could penetrate to the ventral striatum and acutely block KOR but did not produce long-lasting receptor inactivation at VTA dopamine terminals.

Covalent inactivation of KOR by β-chlornaltrexamine effectively blocked KOR signaling for up to a week. To test if a higher rate of receptor recycling in the terminals as compared to cell bodies explained the shortened duration of action of norBNI in dopamine terminals, we used β-chlornaltrexamine (β-CNA) to block opioid signaling. β-CNA is a nitrogen mustard analog of naltrexone that covalently binds to the ligand binding site in the opioid receptor to irreversibly prevent agonist occupation (Schoenecker et al., 1987). ICV injection of 1 µg β-CNA significantly blocked KOR agonist-mediated inhibition of dopamine release from dopamine terminals after either 48 hours or one-week post injection (Figure 2E,F) (One-way ANOVA F = 7.545, p = 0.0067, Tukey's post-hoc Sham vs 48-hour p = 0.009, Sham vs. 1 week p = 0.0129).

Because β-CNA effectively blocked KOR signaling a week post-treatment, faster receptor turnover in dopamine nerve terminals cannot explain the lack of long-lasting norBNI antagonism.

NorBNI antagonism of U69,593 mediated activation of GIRK currents persists up to a week in dopamine cell bodies. The lack of long-lasting norBNI effects in dopamine terminals raises the possibility that the cellular machinery for long-lasting inactivation by norBNI is not expressed by dopamine neurons. To address this, as well as any concerns that slice preparation itself disrupts the norBNI receptor inactivation, we tested whether norBNI produced a long-lasting inhibition of the physiological responses to KOR activation evident in the cell bodies of dopamine neurons. KOR agonists, like other Gi/o-coupled receptors can acutely reduce the excitability in the somatodendritic compartment by increasing conductance of GIRK channels, and norBNI has been previously shown to acutely block this response in VTA dopamine neurons (Margolis et al., 2006).

We injected mice with 10 mg/kg norBNI or saline one week prior to in vitro electrophysiological recording. Dopamine neurons, identified using tdTomato reporter expression in DAT-IRES-cre mice (Figure 3A), consistently showed an increase in the BaCl-sensitive GIRK current and membrane conductance following in vitro application of 1 μM U69,593 (Figure 3B) (Paired two-tailed t-test, current at -115 mV: $t_{2.4,9}$, p = 0.0397, conductance: $t_{3,9}$, p = 0.015; n = 8 animals, 10 cells). However, cells from mice pretreated with norBNI 1 week prior to brain dissection showed no significant increase in GIRK current or conductance in response to 1 μM U69,593 (Figure 3C) (Paired two-tailed t-test, current at -115 mV: $t_{0.962,6}$, p = 0.374, conductance: $t_{0.242,6}$, p =

0.817; n = 7 animals, 7 cells). These data show that norBNI does block KOR-mediated

facilitation of somatic GIRK currents in VTA dopamine neurons for at least a week post-

injection. In most VTA dopamine neurons we patched (primarily in the lateral aspect of the VTA

and labeled with DAT-Cre TdTomato fluorescent reporter), we showed potentiated GIRK

current in response to KOR agonists. Because long-lasting KOR inactivation is a consequence of

JNK/PRDX6-mediated ROS generation (Schattauer et al., 2017a), these results suggest that

norBNI may effectively activate this signaling cascade in the cell bodies but not in terminals of

VTA dopamine neurons. The local effects of norBNI have not previously been reported and

suggest that neither the kappa receptors nor the signal transduction mediators can effectively

migrate between somatic and terminal cellular compartments.

We recently developed a virus containing a sensor for H_2O_2 that acts as a proxy for JNK-ROS

activation by KOR (Schattauer et al., 2017a, 2019). To further delineate the differences in KOR

signal transduction in dopamine neuron cell bodies and terminals, and determine if differences in

ROS were responsible for the duration of antagonist action, we measured the ROS generation

stimulated by KOR agonist activity. We used the functionally selective KOR agonist nalfurafine

(Schattauer et al., 2017b). Nalfurafine is a better reagent to address these mechanistic questions

because it is a KOR agonist that does not effectively activate p38 MAPK, which inhibits ROS

generation (Schattauer et al., 2019). We have observed that it stimulates ROS to a greater extent

than U69,593 and more rapidly than norBNI. As shown in Figure 4A, nalfurafine potently

inhibited the release of dopamine with a logEC50 of -8.54 (95% CI -8.72 to -8.33) (equivalent to

2.9 nM). Nalfurafine was approximately 10-fold more potent than U69,593, with comparable

efficacy (Figure 4A). To visualize neuronal ROS dynamics (Figure 4B), we recorded

20

fluorescence emitted from the virally encoded ROS indicator, AAV-DIO-HyPerRed selectively

expressed in VTA dopamine neurons. The HyPerRed protein has two cysteines with exposed

thiol groups attached to a red fluorescent protein. When the two thiol groups are oxidized in the

presence of H_2O_2, they form a reversible disulfide bond that in turn causes a ratiometric increase

in fluorescence; measuring this fluorescence change provides a measure of the relative change in

H_2O_2 (Ermakova et al., 2014).

As imaged in live brain slices, VTA dopamine neurons in DAT-IRES-Cre mice express the

HyPerRed protein (Figure 4C). Fluorescence intensity was significantly increased by 100 nM

nalfurafine as shown in these representative images (Figure 4C). To confirm HyPerRed

sensitivity, slices were treated with 200 μM H_2O_2 after opioid exposure (Figure 4C&E, right

panels). Nalfurafine caused a consistent, slow onset ~15% increase in the HyPerRed signal in

VTA dopamine neurons, with a peak about 25 minutes after the onset of drug perfusion (Figure

4D). The nalfurafine-induced increase in HyPerRed fluorescence in VTA cell bodies was not

evident in slices pretreated with the non-selective opioid receptor antagonist naloxone (10 μM)

(Figure 4C,D). Both naloxone-nalfurafine and vehicle-nalfurafine samples showed an increased

HyPerRed fluorescence signal in response to 200 μM H_2O_2 (Panel 3 of Figure 4 C,E). Dopamine

terminals in the nucleus accumbens of *in vitro* midbrain slices also expressed the HyPerRed

construct and responded to 200 μM H_2O_2 treatment (Figure 4 E); however, no significant

increase in HyPerRed fluorescence in response to nalfurafine was observed in dopamine

terminals (Figure 4 E,F).

Discussion

In this study, we found that norBNI is an effective long-acting antagonist in female mice, when given in repeated, low-doses. However, like unbiased KOR agonists, norBNI signaling is disrupted by GRK2-mediated phosphorylation in female mice, likely due to high levels of estradiol. We also found that norBNI effectively blocks KOR activation of GIRK currents in dopamine cell bodies for a week after pre-treatment. However, norBNI does not produce a long-lasting block of KOR-mediated inhibition of presynaptic dopamine terminals. This is in contrast to the long-lasting effects of norBNI in serotonergic terminals (Schindler et al., 2012). Together these data emphasize the importance of somatic KOR on VTA dopamine in mediating the behavioral effects of stress. We also found that nalfurafine, a KOR-agonist used to treat pain and itch in humans without psychotomimetic effects or dysphoria (Endoh et al., 2000; Inui, 2015) inhibits dopamine release with higher potency than U50,488, despite its inability to generate aversion or dysphoria. These data further emphasize that presynaptic inhibition of dopamine alone is not sufficient to generate conditioned place aversion or dysphoria in response to KOR agonists.

We found that norBNI is not long-lasting in female mice, unless they are pretreated with CMPD101. This indicates that, as with KOR agonists, interaction between increased estradiol level and GRK2/3 signaling may disrupt the collateral-agonist activity of norBNI in activating JNK. Animals pretreated with norBNI alone had more variance in their tail-flick response, indicating this likely is an estrous dependent effect as was found for agonist active KOR responses in female mice (Abraham et al., 2018b). We also would expect, due to this sex difference, that all long-acting JNK-dependent antagonists, including JDTic would not work in females during high-estradiol periods of their cycles. We would predict that in humans, JNK-

dependent antagonists would potentially be more effective in people taking estradiol-suppressing medications, in menopause, or if taken during low-estrogen points in cycle, which are easier to determine in humans than mice. Regardless, repeated low-dose is a more effective dosing regimen because it reduces compliance issues of missing a single dose without as many potential off target effects of a single high-dose of norBNI (Chavkin et al., 2019). This repeated dosing attenuates the sex difference in norBNI's action. It will be important to further assess the effectiveness of low-dose repeated norBNI at blocking behavioral effects of stress such as immobility in forced swim test, especially in females (Laman-Maharg et al., 2019)

Our finding that norBNI acts as a long acting antagonist blocking the analgesic effects of KOR recapitulate previous results. However, the finding that norBNI does not block KOR-inhibition of dopamine terminals is novel and contributes to both our understanding of collateral agonism by compounds like norBNI and subcellular signaling differences. We believe this effect may be restricted not just to terminals, but specifically dopamine neurons. Previous work demonstrated that pretreatment with norBNI 5 days prior blocks the KOR-mediated increase in SERT translocation to the membrane in serotonin terminals in the nucleus accumbens (Schindler et al., 2012). We originally predicted that the balance of receptors recycling to the membrane after endocytosis and proteolysis may differ in terminals, leading to sufficient degradation and replacement of KOR in presynaptic terminals that after a week, there were no longer enough "locked" receptors to block inhibition. However, the finding that β-Chlornaltrexamine effectively attenuates KOR inhibition of dopamine release for a week disproves this hypothesis. As such, we predict that this indicates there are differences in the signaling effects of norBNI's collateral agonist activity specifically in dopamine presynaptic terminals. This prediction is

further confirmed by the lack of ROS generation in response to nalfurafine in dopamine presynaptic terminals, as compared to the response within the ventral tegmental area.

We did previously show that norBNI can cause a cross-inactivation of the D2 receptor, in dopamine terminals, indicating some amount of receptor inactivation (Schattauer 2017a), but these effects were only measurable in slices taken within an hour of norBNI treatment, indicating that a small, ROS effect may occur, but that it is not sufficient to cause long-lasting inactivation. Dopamine terminals may be either too inundated by ROS, or may too tightly regulate ROS to facilitate JNK-dependent ROS signaling. In a small subcompartment with higher ROS production, the additional ROS generation from norBNI activation of JNK may not be effective to cause depalmitoylation of G proteins and would not be detectable above baseline values, as measured by HyPerRed. One potential explanation for the inability of norBNI to be long-acting at dopamine terminals is that the biochemical environment is less conducive to ROS-mediated signaling (Smythies, 2000; Stokes et al., 1999). The metabolism of dopamine by monoamine oxidase produces reactive hydrogen peroxide as a byproduct and dopamine can become oxidative itself by generation of dopamine-o-quinone (Stokes et al., 1999). Additionally, dopamine neurons have been shown to have more active innate antioxidant activity to counteract ROS generation by catecholamine metabolism (Smythies, 2000). Although we hoped that treatment of slices with sodium ascorbate and thiourea would abrogate these concerns, it is still possible that the ROS levels in dopamine terminals are already too efficiently suppressed to be detected by a cytosolic sensor. Further development of the HyPerRed or related sensors to be membrane targeted may improve our signal to noise in such ROS-sensitive neurons.

In addition to our findings demonstrating the heterogeneity of signaling between cell compartments, the finding that norBNI does not have a long-lasting effect on presynaptic inhibition of dopamine release by KOR generates several key predictions about animal behavior. It has been previously shown that dysphoric components of stress that lead to conditioned avoidance and potentiation of preference for a drug reward depend on KOR on dopamine neurons. norBNI blocks conditioned place aversion to a KOR agonist (5), and the data presented here indicate that this effect cannot be attributed to inhibition of dopamine release. This is further supported by the fact that p38 MAPK is necessary for the aversive effects of KOR, but not necessary for presynaptic inhibition of KOR. Pretreatment with norBNI produces a long-lasting block on increased swim immobility and stress-enhanced cocaine CPP (Laman-Maharg et al., 2018; Chartoff et al., 2012*)*, indicating that presynaptic inhibition of dopamine release is not sufficient to cause these effects. As such, we predict that blockade of kappa opioid receptors in NAc terminals alone would not be sufficient to block behavioral effects of KOR on mood and drug seeking. These findings lead us to predict that G-biased agonists would not be able to produce conditioned place aversion or potentiate drug reward, but would still inhibit dopamine release. Further studies should try to delineate the molecular mechanisms of presynaptic inhibition by KOR to better separate the functional role of this robust physiological effect.

Author Contributions

Participated in research design: Reichard, Land, and Chavkin

Conducted experiments: Reichard, Newton, Rivera, Land, Sotero de Menezes, Schattauer

Performed data analysis: Reichard, Newton, Land, Schattauer

Wrote or contributed to the writing of the manuscript: Reichard, Chavkin

References

Abraham AD, Fontaine HM, Song AJ, Andrews MM, Baird MA, Kieffer BL, Land BB and Chavkin C (2018a) κ-Opioid receptor activation in dopamine neurons disrupts behavioral inhibition. *Neuropsychopharmacology* **43**(2): 362-372.

Abraham AD, Schattauer SS, Reichard KL, Cohen JH, Fontaine HM, Song AJ, Johnson SD, Land BB and Chavkin C (2018b) Estrogen regulation of GRK2 inactivates kappa opioid receptor signaling mediating analgesia, but not aversion. *J Neurosci* **38**(37): 8031-8043.

Becker JB and Chartoff E (2019) Sex differences in neural mechanisms mediating reward and addiction. *Neuropsychopharmacology* **44**(1): 166-183.

Bruchas MR, Yang T, Schreiber S, Defino M, Kwan SC, Li S and Chavkin C (2007) Long-acting kappa opioid antagonists disrupt receptor signaling and produce noncompetitive effects by activating c-Jun N-terminal kinase. *J Biol Chem* **282**(41): 29803-29811.

Buda JJ, Carroll FI, Kosten TR, Swearingen D and Walters BB (2015) A double-blind, placebo-controlled trial to evaluate the safety, tolerability, and pharmacokinetics of single, escalating oral doses of JDTic. *Neuropsychopharmacology* **40**(9): 2059-2065.

Butelman E, Negus S, Ai Y, de Costa B and Woods J (1993) Kappa opioid antagonist effects of systemically administered Nor-Binaltorphimine in a thermal antinociception assay in rhesus monkeys. *Journal of Pharmacology and Experimental Therapeutics* **267**(3): 1269-1276.

Byers SL, Wiles MV, Dunn SL and Taft RA (2012) Mouse estrous cycle identification tool and images. *PLoS One* **7**(4): e35538.

Carlezon WAJ and Krystal AD (2016) Kappa-opioid antagonists for psychiatric disorders: from bench to clinical trials. *Depress Anxiety* **33**(10): 895-906.

Carroll FI and Carlezon WA (2013) Development of κ opioid receptor antagonists. *Journal of Medicinal Chemistry* **56**(6): 2178-2195.

Carroll I, Thomas JB, Dykstra LA, Granger AL, Allen RM, Howard JL, Pollard GT, Aceto MD and Harris LS (2004) Pharmacological properties of JDTic: a novel kappa-opioid receptor antagonist. *Eur J Pharmacol* **501**(1-3): 111-119.

Chartoff E, Sawyer A, Rachlin A, Potter D, Pliakas A and Carlezon WA (2012) Blockade of kappa opioid receptors attenuates the development of depressive-like behaviors induced by cocaine withdrawal in rats. *Neuropharmacology* **62**(1): 167-176.

Chavkin C, Cohen JH and Land BB (2019) Repeated administration of norbinaltorphimine produces cumulative kappa opioid receptor inactivation. *Front Pharmacol* **10**: 88.

Chefer VI, Bäckman CM, Gigante ED and Shippenberg TS (2013) Kappa opioid receptors on dopaminergic neurons are necessary for kappa-mediated place aversion. *Neuropsychopharmacology* **38**(13): 2623-2631.

Clark JJ, Sandberg SG, Wanat MJ, Gan JO, Horne EA, Hart AS, Akers CA, Parker JG, Willuhn I, Martinez V, Evans SB, Stella N and Phillips PEM (2010) Chronic microsensors for

longitudinal, subsecond dopamine detection in behaving animals. *Nat Methods* **7**(2): 126-129.

Daaka Y, Pitcher JA, Richardson M, Stoffel RH, Robishaw JD and Lefkowitz RJ (1997) Receptor and Gβγ isoform-specific interactions with G protein-coupled receptor kinases. *Proc Natl Acad Sci U S A* **94**(6): 2180-2185.

DeVos SL and Miller TM (2013) Direct intraventricular delivery of drugs to the rodent central nervous system. *Journal of Visualized Experiments: JoVE*(75):e50326.

Di Chiara G and Imperato A (1988) Opposite effects of mu and kappa opiate agonists on dopamine release in the nucleus accumbens and in the dorsal caudate of freely moving rats. *Journal of Pharmacology and Experimental Therapeutics* **244**(3) 1067-1080.

Dominguez R, Hu E, Zhou M and Baudry M (2009) 17beta-estradiol-mediated neuroprotection and ERK activation require a pertussis toxin-sensitive mechanism involving GRK2 and beta-arrestin-1. *J Neurosci* **29**(13): 4228-4238.

Ehrich JM, Messinger DI, Knakal CR, Kuhar JR, Schattauer SS, Bruchas MR, Zweifel LS, Kieffer BL, Phillips PEM and Chavkin C (2015) Kappa opioid receptor-induced aversion requires p38 MAPK activation in VTA dopamine neurons. *J Neurosci* **35**(37): 12917-12931.

Endoh T, Tajima A, Suzuki T, Kamei J, Suzuki T, Narita M, Tseng L and Nagase H (2000) Characterization of the antinociceptive effects of TRK-820 in the rat. *European Journal of Pharmacology* **387**(2) 133-140.

Ermakova YG, Bilan DS, Matlashov ME, Mishina NM, Markvicheva KN, Subach OM, Subach FV, Bogeski I, Hoth M, Enikolopov G and Belousov VV (2014) Red fluorescent genetically encoded indicator for intracellular hydrogen peroxide. *Nature Communications* **5:**5222.

Fisher AB (2011) Peroxiredoxin 6: a bifunctional enzyme with glutathione peroxidase and Phospholipase A_2 activities. *Antioxidants & redox signaling* **15**(3): 831-844.

Franklin K and Paxinos G (2008a) *The Mouse Brain in Stereotaxic Coordinates*. 3 ed.

Guerrero M, Urbano M, Kim EK, Gamo AM, Riley S, Abgaryan L, Leaf N, Van Orden LJ, Brown SJ, Xie JY, Porreca F, Cameron MD, Rosen H, Roberts E. (2019) Design and Synthesis of a Novel and Selective Kappa Opioid Receptor (KOR) Antagonist (BTRX-335140). J Med Chem. 62(4):1761-1780.

Horan P, Taylor J, Yamamura H and Porreca F (1992) Extremely long-lasting antagonistic actions of Nor-Binaltorphimine (nor-BNI) in the mouse tail-flick test. *Journal of Pharmacology and Experimental Therapeutics* **260**(3): 1237-1243.

Inui S (2015) Nalfurafine hydrochloride to treat pruritus: A review. *Clinical, cosmetic and investigational dermatology* **8:** 249-255.

Jarman SK, Haney AM and Valdez GR (2018) Kappa opioid regulation of depressive-like behavior during acute withdrawal and protracted abstinence from ethanol. *PLoS One* **13**(9): e0205016.

Kenakin T (2005) New concepts in drug discovery: collateral efficacy and permissive
antagonism. *Nature reviews Drug discovery* **4**(11) 919-927.

Laman-Maharg A, Williams AV, Zufelt MD, Minie VA, Ramos-Maciel S, Hao R, Ordones
Sanchez E, Copeland T, Silverman JL, Leigh A, Snyder R, Carroll FI, Fennell TR and
Trainor BC (2018) Sex differences in the effects of a kappa opioid receptor antagonist in
the forced swim test. *Front Pharmacol* **9**: 93.

Leander JD (1988) Buprenorphine is a potent kappa-opioid receptor antagonist in pigeons and
mice. *European Journal of Pharmacology* **151**(3): 395-402.

Lemos JC, Wanat MJ, Smith JS, Reyes BAS, Hollon NG, Van Bockstaele EJ, Chavkin C and
Phillips PEM (2012) Severe stress switches CRF action in the nucleus accumbens from
appetitive to aversive. *Nature* **490**(7420): 402-406.

Lowe JD, Sanderson HS, Cooke AE, Ostovar M, Tsisanova E, Withey SL, Chavkin C,
Husbands SM, Kelly E, Henderson G and Bailey CP (2015) Role of G Protein-Coupled
Receptor Kinases 2 and 3 in mu-opioid receptor desensitization and internalization. *Mol
Pharmacol* **88**(2): 347-356.

Margolis EB, Lock H, Chefer VI, Shippenberg TS, Hjelmstad GO and Fields HL (2006) Kappa
opioids selectively control dopaminergic neurons projecting to the prefrontal
cortex. *Proceedings of the National Academy of Sciences of the United States of
America* **103**(8): 2938-2942.

Melief EJ, Miyatake M, Carroll FI, Béguin C, Carlezon WA, Cohen BM, Grimwood S, Mitch
CH, Rorick-Kehn L and Chavkin C (2011) duration of action of a broad range of
selective κ-opioid receptor antagonists is positively correlated with c-Jun N-Terminal
Kinase-1 activation. *Mol Pharmacol* **80**(5): 920-929.

Rice ME (1999) Use of ascorbate in the preparation and maintenance of brain slices. *Methods
(San Diego, Calif)* **18**(2): 144-149.

Rorick-Kehn LM, Witcher JW, Lowe SL, Gonzales CR, Weller MA, Bell RL, Hart JC, Need
AB, McKinzie JH, Statnick MA, Suico JG, McKinzie DL, Tauscher-Wisniewski S,
Mitch CH, Stoltz RR and Wong CJ (2014) Determining pharmacological selectivity of
the kappa opioid receptor antagonist LY2456302 using pupillometry as a translational
biomarker in rat and human. *International Journal of Neuropsychopharmacology* **18**(2):
pyu036.

Schattauer SS, Bedini A, Summers F, Reilly-Treat A, Andrews MM, Land BB and Chavkin C
(2019) Reactive Oxygen Species (ROS) generation is stimulated by κ opioid receptor
activation through phosphorylated c-Jun N-terminal kinase and inhibited by p38
mitogen-activated protein kinase (MAPK) activation. *Journal of Biological
Chemistry* **294**(45): 16884-16896.

Schattauer SS, Kuhar J, Song A and Chavkin C (2017a) Nalfurafine Is a G-protein biased
agonist having significantly greater bias at the human than rodent form of the kappa
opioid receptor. *Cellular Signalling* **32:** 59-65.

Schattauer SS, Land BB, Reichard KL, Abraham AD, Burgeno LM, Kuhar JR, Phillips PEM, Ong SE and Chavkin C (2017b) Peroxiredoxin 6 mediates Galphai protein-coupled receptor inactivation by cJun kinase. *Nat Commun* **8**(1): 743.

Schindler AG, Messinger DI, Smith JS, Shankar H, Gustin RM, Schattauer SS, Lemos JC, Chavkin NW, Hagan CE, Neumaier JF and Chavkin C (2012) Stress produces aversion and potentiates cocaine reward by releasing endogenous dynorphins in the ventral striatum to locally stimulate serotonin reuptake. *J Neurosci* **32**(49): 17582-17596.

Schoenecker J, Takemori A and Portoghese P (1987) Opioid agonist and antagonist activities of monofunctional nitrogen mustard analogues of Beta-chlornaltrexamine. *Journal of Medicinal Chemistry* **30**(5): 933-935.

Shirayama Y, Ishida H, Iwata M, Hazama GI, Kawahara R and Duman RS (2004) Stress increases dynorphin immunoreactivity in limbic brain regions and dynorphin antagonism produces antidepressant-like effects. *J Neurochem* **90**(5): 1258-1268.

Smith C, Medzihradsky F, Hollingsworth P, DeCosta B, Rice K and Woods J (1990) Nor-binaltorphimine is a reversible, noncompetitive opioid antagonist in the mouse vas deferens with high affinity for kappa receptors in monkey brain membranes. *Progress in Clinical and Biological Research* **328**: 65-68.

Smythies J (2000) Redox aspects of signaling by catecholamines and their metabolites. *Antioxidants & Redox Signaling* **2**(3):573-583.

Stokes AH, Hastings TG and Vrana KE (1999) Cytotoxic and genotoxic potential of

dopamine. *Journal of Neuroscience Research* **55**(6): 659-665.

Thal DM, Yeow RY, Schoenau C, Huber J and Tesmer JJG (2011) Molecular mechanism of

selectivity among G protein-coupled receptor kinase 2 inhibitors. *Mol Pharmacol* **80**(2):

294-303.

Ting JT, Daigle TL, Chen Q and Feng G (2014) Acute brain slice methods for adult and aging

animals: application of targeted patch clamp analysis and optogenetics. *Methods in*

Molecular Biology (Clifton, NJ) **1183**: 221-242.

Williams JT, North RA and Tokimasa T (1988) Inward rectification of resting and opiate-

activated potassium currents in rat locus coeruleus neurons. *J Neurosci* **8**(11): 4299-

4306.

Footnotes

Legends

Figure 1 – Long-acting norBNI antagonism in females is effective if given in repeated doses

or after CMPD101. *Note: all groups are independent studies with unique control group, each*

experiment is separated by a dashed line. They are shown as maximum possible effect (%MPE),

to compare across groups. Error bars of variability shown are Standard Deviations of the

means. A. Male mice were injected with either saline or 10 mg/kg norBNI (i.p.). One week later

they were injected with 10 mg/kg U50,488 and tested for a shift in tail withdrawal latency after

immersion in 52.5^{o}C water. Male mice pretreated with norBNI did not show a significant

increase in tailflick latency, but those pretreated with saline did. (Unpaired two-tailed t-test, one-

tailed: $t_{2.916,18}$ p=0.0092) B. *F*emale mice did not show an increased latency to flick after

U50,488 treatment (data reprinted from Abraham et al 2019), but did after pretreatment with

CMPD101(15 mg/kg), U50,488. C. One-week pretreatment with either CMPD101 alone or

norBNI alone did not affect U50,488 increase in tail-flick latency, but treating mice with

CMPD101 prior to norBNI led to a long-acting block of the U50,488 increase in tail-flick latency

(One-Way ANOVA F = 5.316, p=0.0242; Tukey's post-hoc CMPD101-vehicle vs. CMPD101-

norBNI p=0.0215). D. Female mice treated with repeated saline injections showed an increase in

tail-flick latency to CMPD101 plus U50,488, but those treated with repeated norBNI doses did

not. (Unpaired two-tailed t-test: $t_{2.607,11}$ p=0.0204) (Each group separated by dotted lines was

normalized to the max possible effect within the group. Error bars indicate standard deviation.

All groups were compared using a one way ANOVA p < 0.05; post-hoc Bonferonni *,**

indicates p<0.05, p<0.01). E. Western blot immunoreactivity to phospho-JNK and actin control

35

in striatal amples taken from mice pretreated with either CMPD101 or vehicle then given vehicle

or norBNI, 60 minutes prior to sac. F. Quantitation of Western blot IR demonstrating that

norBNI caused a significant increase in striatal phospho-JNK in female mice pretreated with

CMPD101, but not in mice pretreated with saline (Two-Way ANOVA with Sidak post-hoc, **

indicates $p < 0.01$).

**Figure 2 – norBNI does not cause a long-lasting block of KOR inhibition of dopamine

release in the nucleus accumbens (NAc) core, whereas β-CNA receptor inactivation persists

at least a week in NAc terminals.** (A,B,C) Example traces demonstrating evoked dopamine

release in response to a 120-180 µA electrical stimulation before (black) and after (grey)

washing on KOR agonist U69,593 (1 µM) in animals who had either been pre-treated with an IP

injection of saline or norBNI prior to brain dissection and tissue sectioning. D. U69,593 inhibits

dopamine release in NAc core slices, and this effect was significantly attenuated by pretreatment

with norBNI one hour prior to slicing, but not by 24 hour or one-week pretreatment with norBNI

(One Way ANOVA $p < 0.05$, post-hoc saline vs. 1-hour $p < 0.01$; error bars indicated standard

deviation). E. Example traces of evoked dopamine before and after U69,593 in sham pretreated

animals. F. Intracerebro-ventricular (IVC) injection of 1 µg β-Chlornaltrexamine significantly

attenuated the effect of U69,593 on inhibition of dopamine release (One-Way ANOVA $p < 0.01$;

Sham vs 1 week $p < 0.05$, Sham vs 48 hr $p < 0.01$; error bars indicated standard deviation)

Figure 3 – **KOR Agonist U69,593 Activates a GIRK current in VTA dopamine neurons that can be blocked by norBNI pretreatment A.** Fluorescent cells in the VTA DAT-ires-cre Flox-tdTomato mice were patched and held at -60 mV. GIRK currents were elicited by subjecting the cells to a voltage ramp from -120 mV to -50 mV. B. GIRK current at baseline and in response to 1 μM U69,593: example trace, current at -115 mV, and conductance. Treatment with the KOR agonist significantly increased GIRK currents (paired two-tailed t-test, $p < 0.05$) and conductance as calculated by the slope of the line from -120 mV to -50 mV (paired two-tailed t-test, $p < 0.05$). C. GIRK currents as measured at baseline and after U69,593 from animals pretreated with: example trace, current at -115 mV, and conductance. D. Peak current after U69,593 minus peak current at baseline denoted as "ΔpF after U69,593" is significantly different in controls as compared to animals pretreated with norBNI. (Unpaired two-tailed t-test * indicates $p < 0.05$; error bars indicated standard deviation).
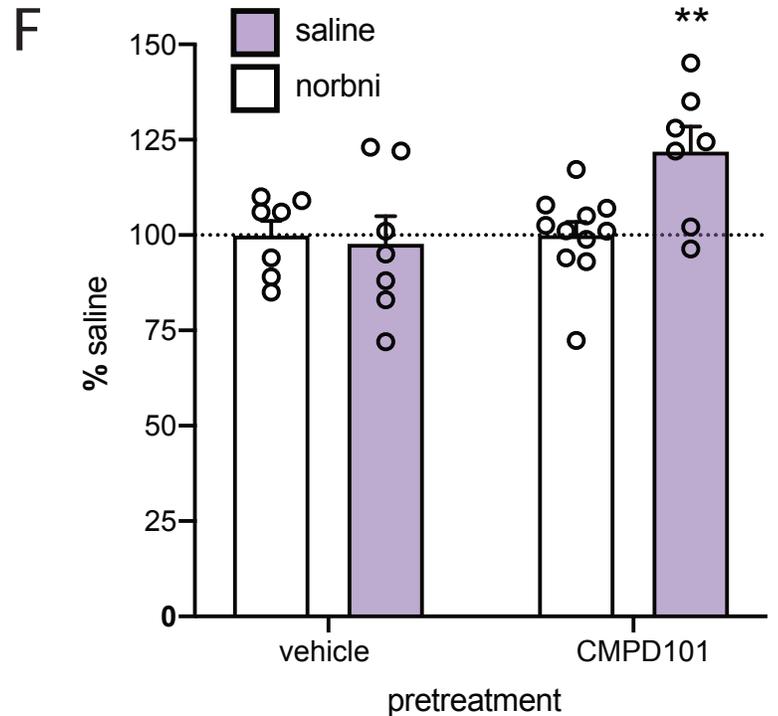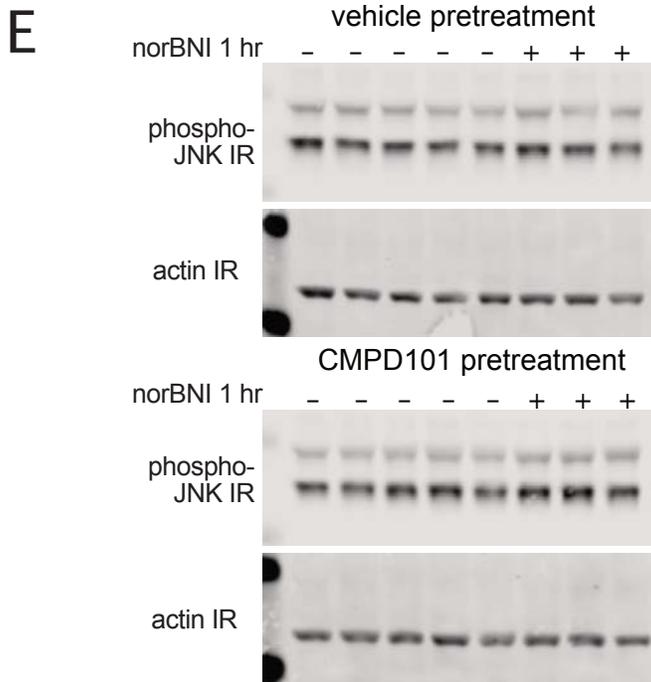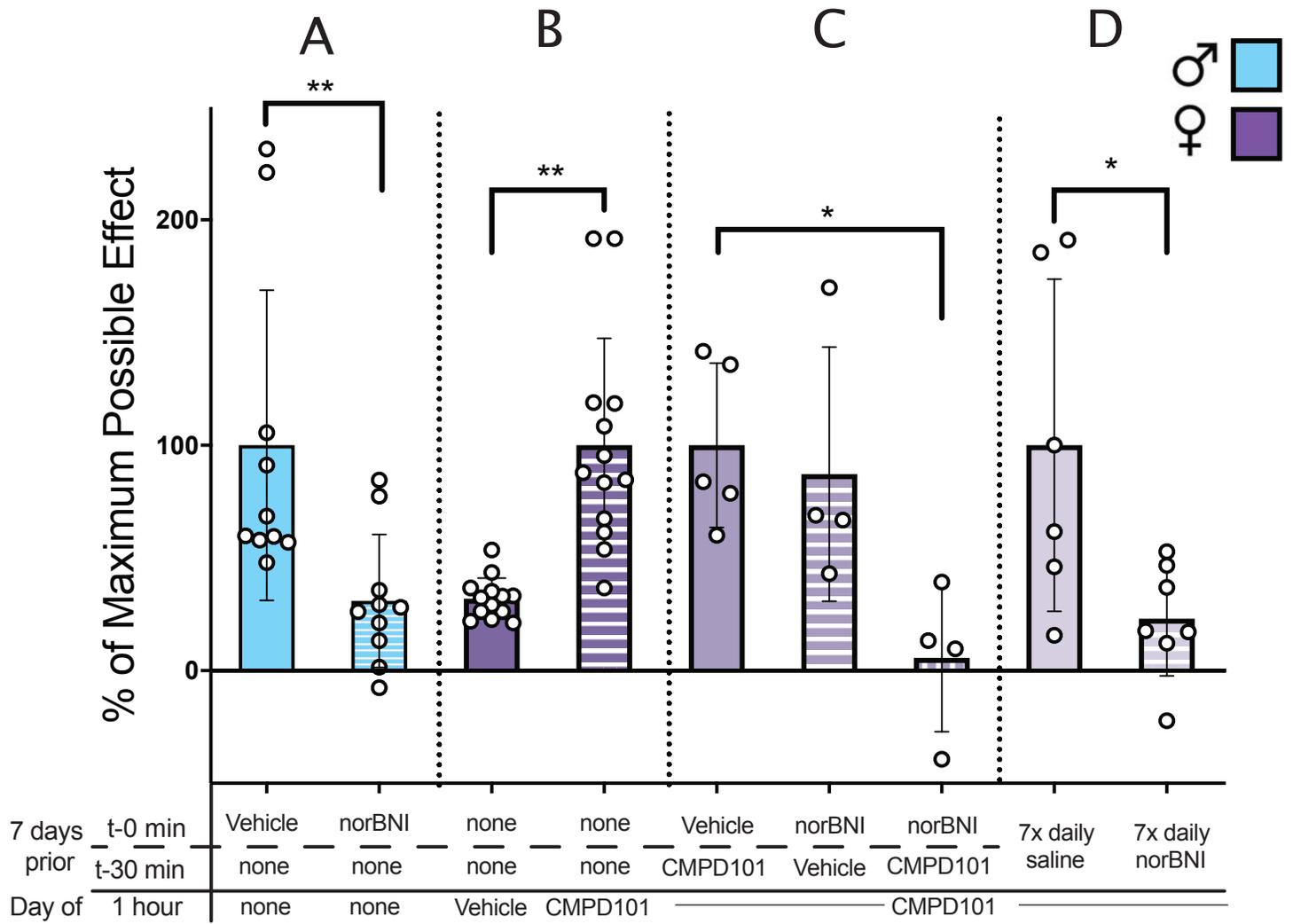
Figure 4 KOR agonist, nalfurafine, generates reactive oxygen species in VTA Dopamine cell bodies, but not dopamine terminals in the nucleus accumbens, as measured by HyPerRed.

A. Nalfurafine and U69,593 dose-dependently inhibit electrically evoked dopamine release in the nucleus accumbens. Nalfurafine is more potent than the agonist U69,593 ($logEC_{50}$•Nalfurafine = -8.54 vs. $logEC_{50}$•U69,593 = -7.72). B. Nalfurafine preferentially activates the G-protein mediated signaling at the KOR receptor, including dopamine inhibition *and* JNK signaling, allowing us to confirm if the JNK-ROS signaling also activated by norBNI is occurring in dopamine neurons. C. VTA dopamine neurons HyPerRed fluorescence response pseudocolored in "Red Hot" in FIJI to represent intensity. Cells with clear nalfurafine and H_2O_2 responses

37

indicated with carat (scale = 100 µm) In all groups tested, 200 µM H2O2 was applied after

agonist treatment. D. Oxygenated aCSF was perfused at 2 ml/min over sections, with images

every two minutes. At t = -7 naloxone was washed onto naloxone-nalfurafine slices. At t = 0,

aCSF with 100 nM nalfurafine was washed over slices. At ~20 min post-nalfurafine wash-on,

VTA HyPerRed fluorescence begins to increase. This persists for ~15 minutes. Images were

taken every two minutes. The nalfurafine group was significantly different from the naloxone-

nalfurafine group at t = 28-34 (Two-Way ANOVA $F_{(23, 69)} = 4.815$, $p < 0.0001$. Sidak post-

hoc, time of 27,35 $p<0.05$, time of 29-33 $p<0.01$). Again, in all groups tested, 200 µM H2O2 was

applied after agonist treatment. E. Comparable recordings of HyPerRed expressing fibers in the -

NAc showed clear H_2O_2 response (scale = 100 µm). F. Neither nalfurafine treated slices or

naloxone-nalfurafine treated slices showed a significant response to nalfurafine (Two-Way

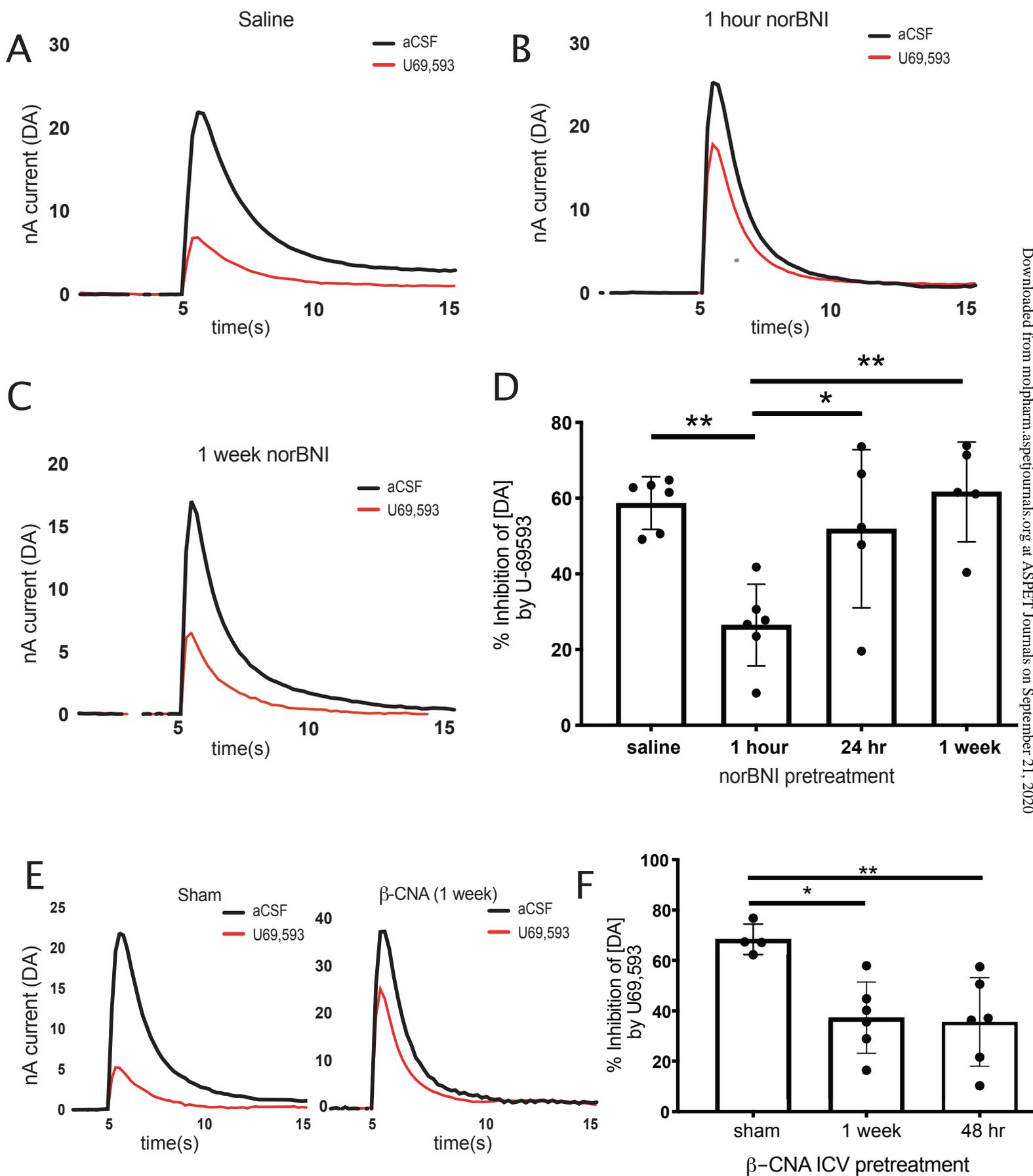ANOVA $F_{(25,150)} = 0.3309$, $p > 0.9$).
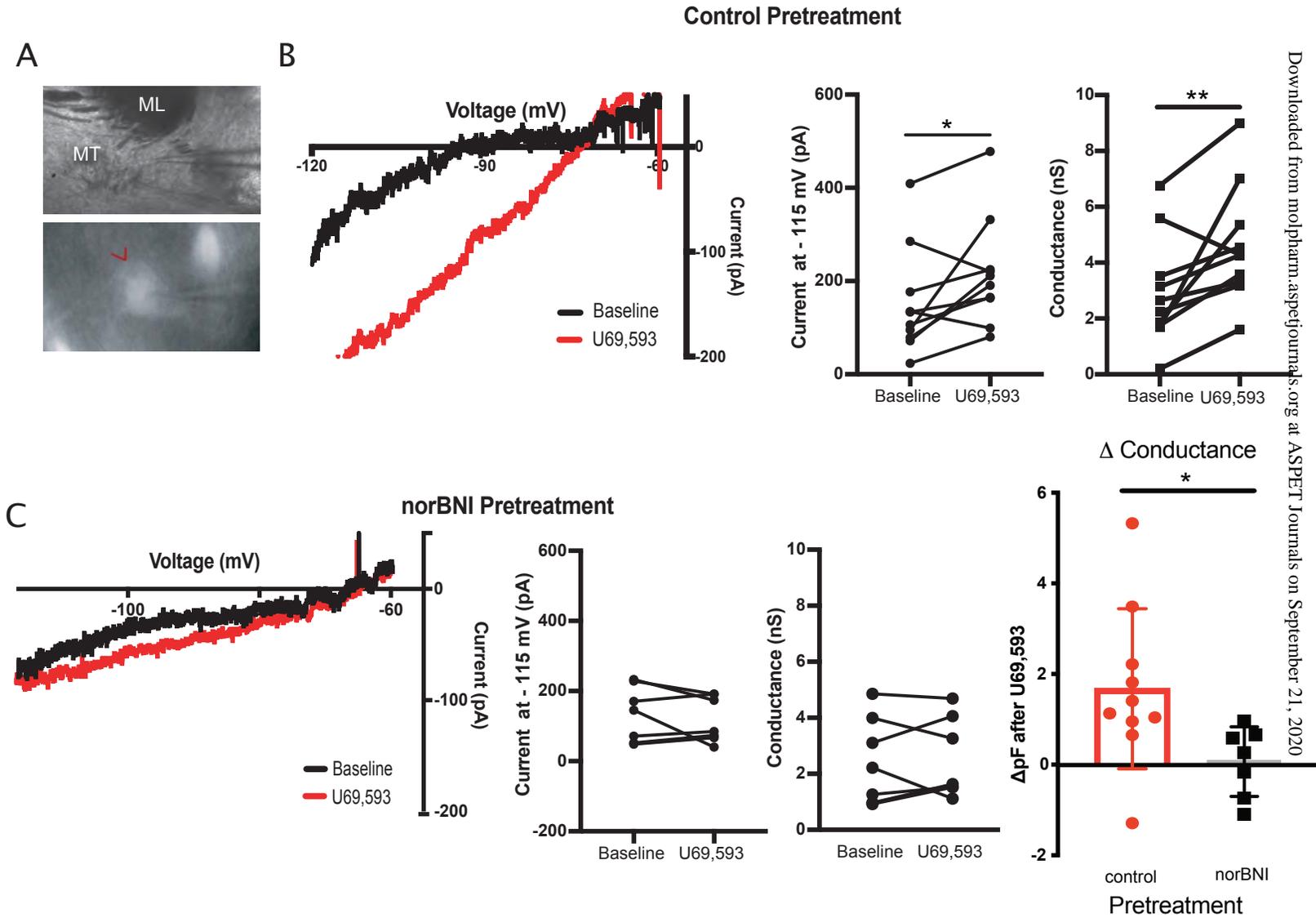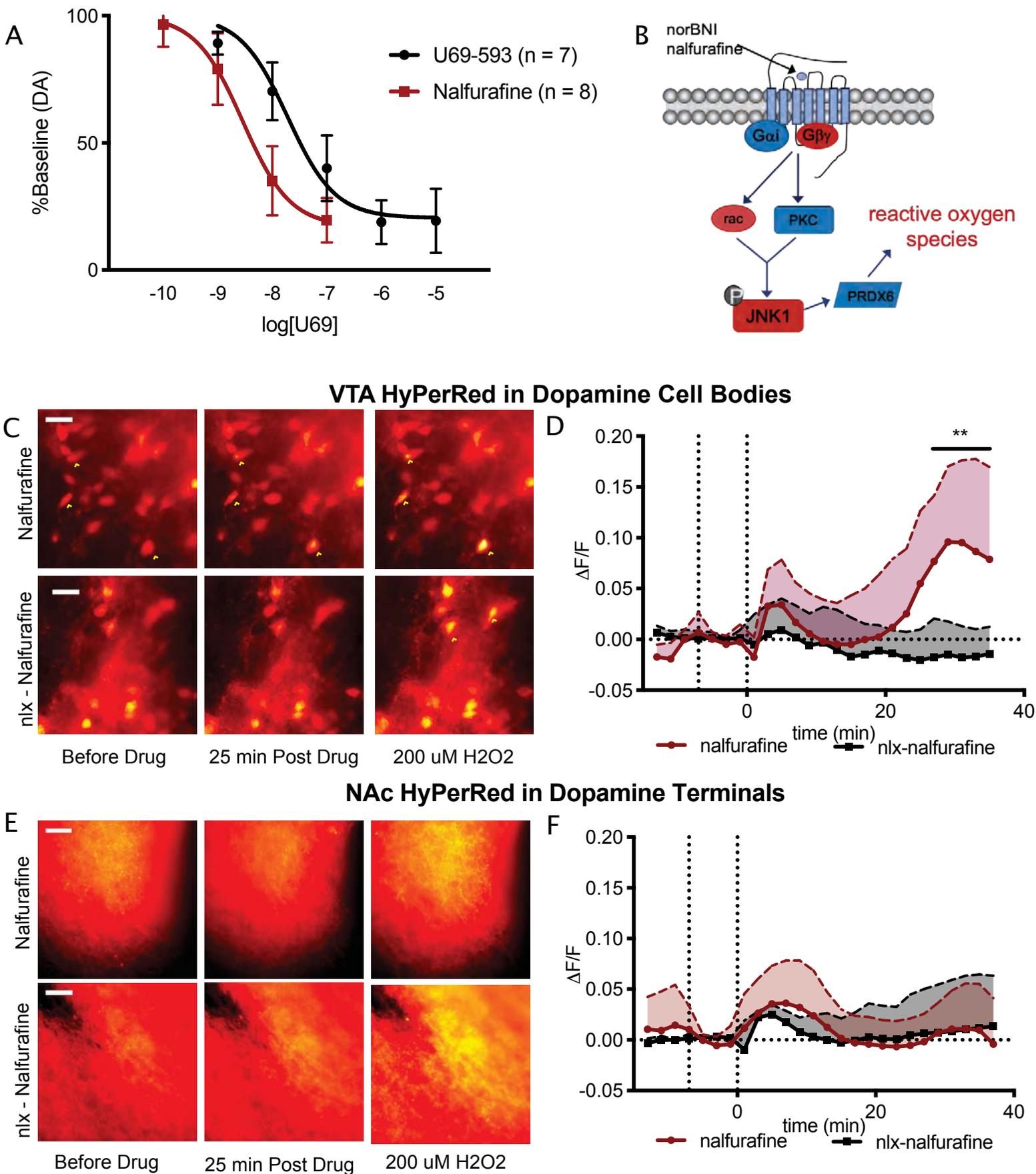
Figure 1

Tail Flick Analgesia

Figure 2

Figure 3

A

B

VTA HyPerRed in Dopamine Cell Bodies

C

D

NAc HyPerRed in Dopamine Terminals

E

F

Figure 4